Toward Multifunctional Polymer Hybrid through Tunable Charge Transfer Interaction of Anthracene/Naphthalenediimide

*Linzhi Zhang, Hongjie Xu, Xiaodong Ma, Zixing Shi, Jie Yin, and Xuesong Jiang**

The interaction between building blocks in the polymer hybrids plays an important role in their performance and functions. Herein, a novel multifunctional polymer hybrid with tunable charge transfer (CT) interaction between π-electron-poor naphthalenediimide (NDI) containing polyimide (PI) and π-electron-rich anthracene (AN) ended polyhedral oligomer silsesquioxane (POSS-AN) is reported (name the polymer hybrid "PI@POSS-AN"), in which the presence of CT interaction between NDI and AN and its controllable feature are confirmed by UV–vis and fluorescence spectra. A new absorption band at 500 nm in the visible region appears and the emission maxima of the CT complexes are distinctly red-shifted to 645 nm, while the fluorescence of NDI (493 nm) and AN (481 nm) are significantly quenched in the polymer hybrids. The resulting hybrid films are transparent and homogeneous, exhibit the enhanced thermal and mechanical performance with the increasing content of POSS-AN. Thanks to the reversible photodimerization of AN, CT interaction between NDI and AN can be *on-off* controlled in situ by UV light and heating, and rewritable fluorescence micro-patterns with red and green emission can be obtained. In addition, the cross-linked polymer hybrids possess healability and reprocessing performance.

1. Introduction

Organic–inorganic hybrids possess superior properties of organic materials (flexibility, easy processing, structural diversity, efficient luminescence, etc.) and inorganic materials (excellent mechanical property, thermal stability, easy to modify, electrical mobility, etc.). The properties of hybrids can be flexibly tuned by combining different organic and inorganic counterparts which provide unlimited possibility to apply in many specific areas.[1–3] Hence, research into organic–inorganic hybrids is booming. Applications of advanced organic–inorganic hybrids have been widely investigated in various fields including environmental monitoring,[4] nanomedicine,[5] biotechnological,[6,7] catalysis,[8] semiconductors,[9,10] photodetectors,[11] optics,[12] and solar cells.[13–15]

Obviously, the properties of organic–inorganic hybrids are not only the sum of the parent constituents, but also the inner interactions between individual building blocks could be predominant. More than that, the interactions make the inorganic and organic materials mixed at the different scale from molecular level to macroscale. According to the nature of the inner interaction, organic–inorganic hybrids can be approximately divided into two distinct types.[1] *Type I* hybrids possess relatively weak interactions between organic and inorganic components. The weak interactions or supramolecular chemistry includes hydrogen bonds, metal–ligand coordination, host–guest interactions, and charge transfer (CT) interactions. In *Type II* hybrids, the two counterparts are linked together via strong chemical bonds (covalent bonds). Compared with strong chemical bonds, the weak interactions in *Type I* hybrids are easier to be regulated. Especially, the strength of some weak interactions can be exactly controlled via appropriate external stimulus such as light[16] and heat.[17] The precise control of interactions could be helpful for preparing various functional materials whose physical and chemical capability, such as luminescence and tensile strength, can be transformed as desired. Additionally, controlling the inner interactions of the composite systems could in turn contribute to interpretation the mechanism and intrinsic quality of the interactions. Therefore, to tune interaction between two components in polymer hybrid is a powerful approach to design and prepare multifunctional materials.

The charge transfer (CT) interactions are indicative of a weak interaction between donors and acceptors.[18,19] As a structural motif, CT complexes usually are analogous to hydrogen-bonded complexes in its complementarities and oriented qualities.[20] Further advantages of CT interactions include easy spectroscopic probing and wider solvent tolerance. Therefore, many procedures have been developed to prepare the functional CT composite materials. Howard's group has prepared a series of healable supramolecular polymer blend by taking advantage of the CT interactions (π–π stacking) between π-electron-rich pyrenyl and

L. Zhang, Prof. H. Xu, X. Ma, Prof. Z. Shi, Prof. J. Yin, Prof. X. Jiang
School of Chemistry and Chemical Engineering
Shanghai Key Laboratory of Electrical Insulation and Thermal Ageing
State Key Laboratory for Metal Matrix Composite Materials
Shanghai Jiao Tong University
Shanghai 200240, P. R. China
E-mail: ponygle@sjtu.edu.cn

DOI: 10.1002/admi.201600224

π-electron-poor naphthalenediimide (NDI) units.[17,21,22] Ono et al. have raised a multimolecular assembly systems by CT interactions, which exhibited guest-dependent color-tunable emissions from deep blue to orange.[23] Guldi's group has reported a range of stable supramolecular donor–acceptor hybrids with particular photophysical features. More recently, they have reported a novel supramolecular CT hybrid which stems from the combination of guanidinium bis-porphyrin tweezers and fullerene carboxylate. The CT interactions between the two parts can strength the overall binding of resulting hybrid, in which a nanosecond-lived radical ion pair state can be generated by excitation.[24,25] These works by means of CT interactions endow the materials with excellent mechanical capacity, optical performance, and electric property. In these current works, however, in situ tuning of CT interaction in hybrid materials is rarely reported.

In this text, we designed an organic–inorganic hybrid material whose inner CT interactions can be *on-off* controlled in situ by ultraviolet radiation and heating. The whole scheme to illustrate the tunable process of CT interactions is shown in **Figure 1**. The CT hybrid was prepared by the combination of organic π-electron-poor NDI backbone contained polyimide (PI) and inorganic π-electron-rich anthracene (AN)-ended polyhedral oligomer silsesquioxane (POSS-AN). NDIs, promising n-type semiconductor materials, are a compact, electron deficient class of aromatic compound capable of being incorporated into larger multicomponent assemblies through intercalation.[26,27] As a nano-sized dimensionally stable cubic silica structure, POSS attracts numerous attention due to its comprehensive application in hybrid materials and can reinforce mechanical strength of the hybrids.[28–30] What's more, POSS can act as large and functional chemical crosslinks when blended with polymer.[31] In the design of POSS-AN, anthracene groups play two different roles: (1) anthracene groups are π-electron-rich and have strong CT interaction with π-electron-poor NDI units, (2) anthracene possesses controllable reversible photodimerization behavior to make the polymer hybrids cross-linked reversibly as desired, consequently resulting in *on-off* control the existence of CT interactions in situ. The tunable CT interactions enable us to obtain fluorescence switchable materials with rewritable function as well as mechanically tough materials with recycling and healing properties.

2. Results and Discussion

2.1. Formation of CT Hybrids

The chemical structures of two components PI and POSS-AN are presented in Figure 1. The samples were prepared by solution casting of mixture of PI and POSS-AN. It is important to yield hybrid materials with a homogeneous dispersion of POSS-AN in the polymer matrix (PI). After blending PI (yellowish-brown, elastomer) with POSS-AN (faint yellow, powder) in chloroform, taking sample PI@POSS-AN/1-1 (weight ratio of POSS-AN is 39%) for example, a deep red, transparent and self-supporting film was obtained. Besides, they also show unique photoluminescence characteristics. Under UV light irradiation, emission color variation was acquired. Green (PI), blue (POSS-AN), and red (PI@POSS-AN/1-1) emissions were observed, as shown in Figure 1b. Hence, it is believed that the existence of the strong CT interaction between NDI and AN leads to mixing of PI and POSS-AN in molecular scale, resulting in the transparent film with new fluorescence emission. In order to explore the CT interaction in the hybrids, we prepare a series of samples (1-0, 16-1, 8-1, 4-1, 2-1, 1-1, 0-1) with different proportion of NDI and AN moieties for the following analysis.

The optical properties of the hybrid films were first studied by absorption and fluorescence spectroscopy. As shown in UV–vis spectra (**Figure 2**), both main absorption bands of PI

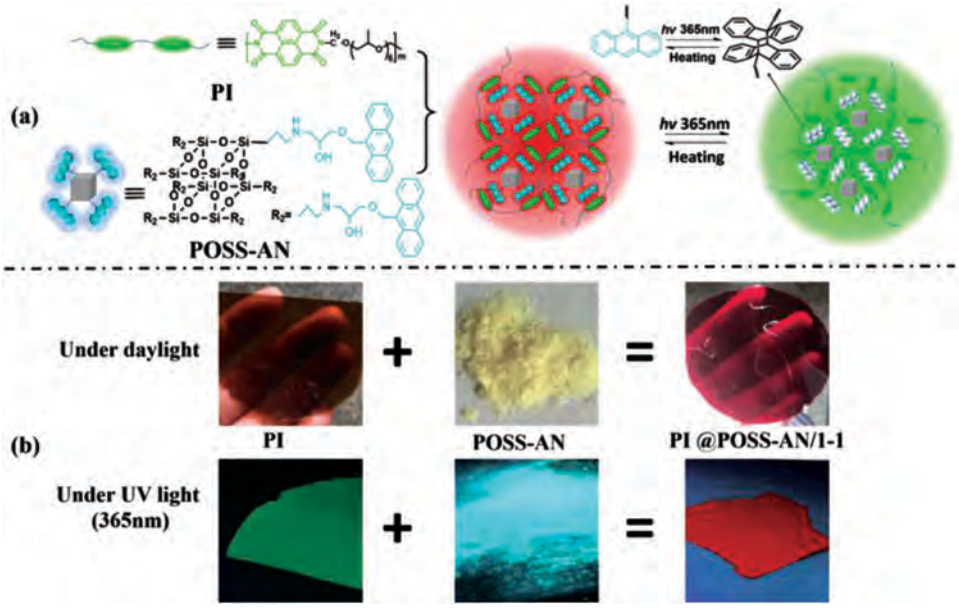

Figure 1. a) Chemical structures of PI and POSS-AN, and schematic illustration of the CT interaction between NDI and AN tuned by the reversible photodimerization of AN; b) Photographs of PI, POSS-AN, and PI@POSS-AN/1-1 hybrid under daylight and UV (365 nm) light.

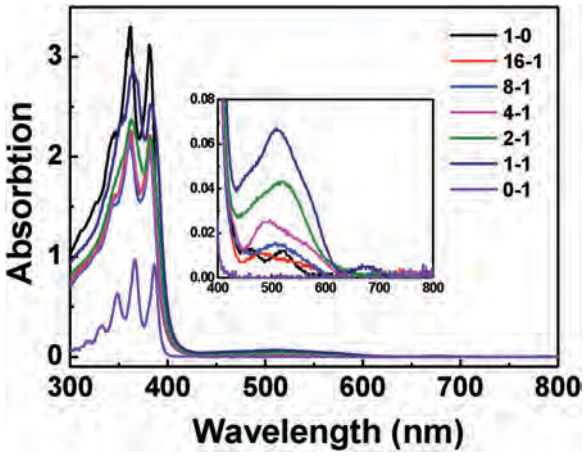

Figure 2. UV–vis absorption spectra of PI@POSS-AN hybrid films with molar ratio between NDI and AN from 1-0 to 0-1.

and POSS-AN locate at 365 nm in the UV region, while a new absorption band at 500 nm in the visible region appears after blended, resulting in the red color appearance of hybrid film. This new bathochromically shifted bands at higher wavelength is an evidence of the CT interaction between PI and POSS-AN.[23,32] The absorption of CT complex at 500 nm was strengthened with the increasing ratio of POSS-AN until 1:1 molar ratio between NDI and AN moieties. Moreover, it can be ascertained that the binding ratio between NDI and AN moieties could be 1:1 according to UV–vis spectra (seen in Figure S1, Supporting Information).

The CT interaction between NDI and AN also leads to the interesting fluorescence emission of the resulting hybrid films. **Figure 3** presents their fluorescence emission spectra and corresponding photographs taken under UV light. The hybrid films show dependent photoluminescence on the molar ratio of NDI and AN, and their color change from light green to deep red with the increasing content of AN. The maxima emission of samples 1-0 (pure PI) and 0-1 (pure POSS-AN) were in 494 nm and 480 nm, respectively. When blended, both fluorescence emissions assigned to NDI and AN were quenched obviously due to the CT interaction between electron-poor NDI and electron-rich AN moieties, while a new peak red-shifted to 650 nm appeared, which should be ascribed to the fluorescence emission of CT complex. The intensity of emission at 650 nm was enhanced gradually along with increasing content of POSS-AN. The fluorescence emission originated from CT complex results in the red appearance of the hybrid films under UV light. In short, the interesting and practically vital photoluminescence characteristics of the hybrids are attributed to the CT interactions.

To gain more insight into the excited state of CT complex and photophysical properties on the emissions of hybrid film, the lifetimes of NDI chromophore (494 nm) were measured, and the corresponding fitted emission decay curves are shown in **Figure 4** (for detailed information see Figure S2 and Table S1, Supporting Information). The fluorescence lifetime ($t_{1/2}$) of NDI chromophore becomes shorter from 2.71 to 0.82 ns along with the addition of POSS-AN. This might be explained by the fact that the excited state of NDI in the hybrid films is quenched due to CT interaction between NDI and AN, resulting in the decreasing fluorescence lifetime.

The formation of CT interaction in the hybrid films leads to the excellent compatibility between PI and POSS-AN, which can be reflected by the transparent, homogeneous appearance of hybrid films even with very high 39 wt% content of POSS-AN. The uniformity of these hybrid films was confirmed by differential scanning calorimetry (DSC) and atomic force microscope (AFM). As shown in **Figure 5**, pure PI takes a glass transition at around 9.2 °C. A small melting peak at –23.5 °C can be found in the DSC curve of PI, which might be ascribed to the melting peak of poly(propylene oxide) (PPO) chains in the backbone of PI. The melting temperature (T_m) of POSS-AN is 73.9 °C. All hybrid films exhibited one glass transition and no melting peak, indicating that two components PI and POSS-AN can mix together in a molecular scale. This should be resulted from the strong CT interaction. With the increasing content of POSS-AN, T_g of hybrid films were enhanced from 9.2 to 30.4 °C. Two reasonable factors might result in the

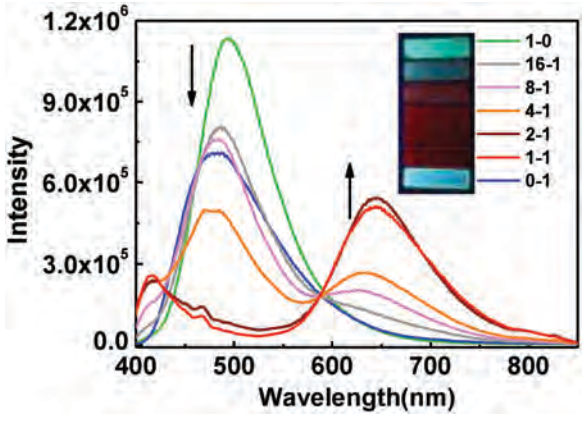

Figure 3. Fluorescence emission spectra of PI@POSS-AN hybrid films with molar ratio between NDI and AN from 1-0 to 0-1 and corresponding photographs taken under UV light (365 nm). Excitation wavelength is 385 nm.

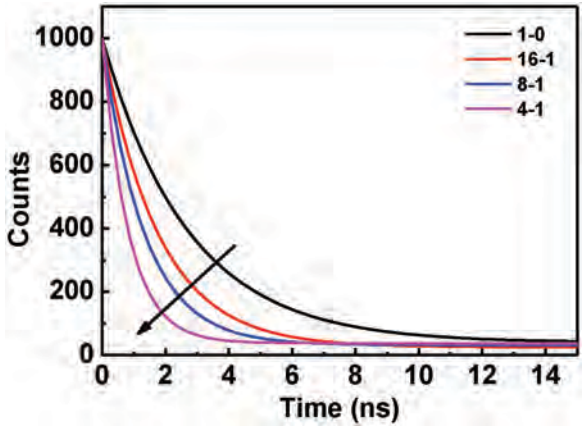

Figure 4. Fitted emission decay curves of PI@POSS-AN hybrid films with molar ratio between NDI and AN from 1-0 to 4-1. The lifetimes of NDI chromophore in samples PI@POSS-AN/2-1 and PI@POSS-AN/1-1 are too short to be measured.

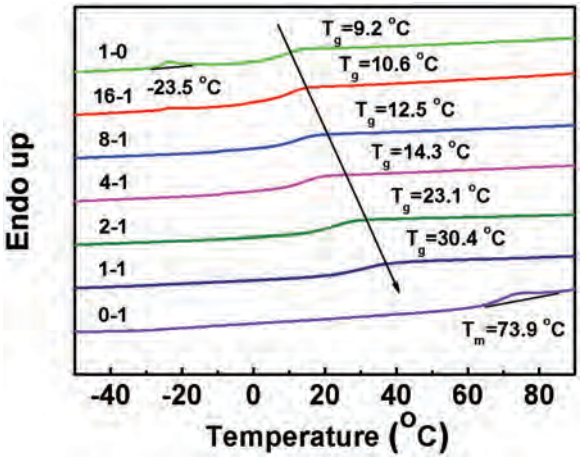

Figure 5. DSC curves of PI @POSS-AN hybrid films with molar ratio between NDI and AN from 1-0 to 0-1 at a scanning rate of 10 °C min^{-1} upon heating.

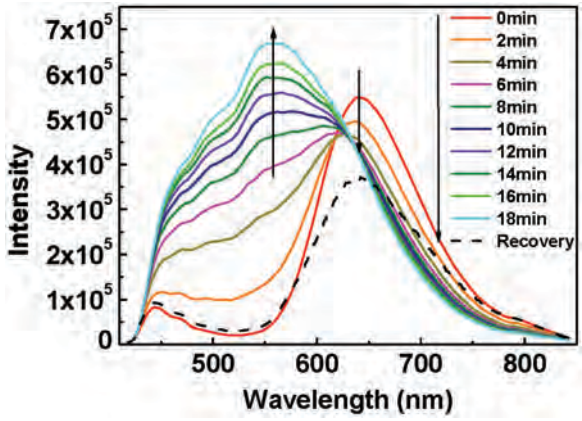

Figure 6. Fluorescence emission spectra of sample PI@POSS-AN/1-1 under different irradiation (365 nm) time. The line "recovery" represents the cross-linked sample PI@POSS-AN/1-1 heated at 150 °C for 3 h.

significantly increasing T_g. One is the rigid cubic silica cage of POSS skeleton. The introduction of POSS can enhance T_g of flexible polymer matrix obviously. The other is the strong CT interaction. The formation of CT complex between NDI and AN moieties in the hybrid film can be considered as physical cross-linking point, which might limit the mobility of PI chain, consequently resulting in the enhancement of T_g. The AFM contrast images exhibited a very homogeneous surface without any noticeable domains, suggesting no obvious phase separation in the hybrid films (Figure S3, Supporting Information).

2.2. Light-Control of the CT Interaction

As a conjugated and planar structure, AN moieties exhibit a reversible photodimerization upon irradiation of light and heating. Due to the unconjugated and unplanar structure, the resulting AN dimer cannot form the CT complex with NDI, leading to no CT interaction. Therefore, the reversible photodimerization of AN might be expected to control the CT interaction between NDI and AN. To verify this point, we used UV–vis adsorption and fluorescence spectra to investigate the CT interaction upon irradiation of UV light (Figure S4, Supporting Information, and **Figure 6**). Generally, CT complexes possess distinct spectroscopic signature such as broad emission bands at higher wavelengths and can be easy for spectrum detecting. As shown in Figure S4 (Supporting Information), the absorption band in the visible region assigned to CT complex decreased along with irradiation of 365 nm UV light, indicating the CT interaction was weakened. This was further confirmed by fluorescence emission spectra shown in Figure 6. The emission around 650 nm related to CT complex was weakened significantly along with the increasing time of UV irradiation, and almost disappeared after irradiation for about 20 min, indicating that photodimerization of AN can *turn-off* the CT interaction between NDI and AN. The weakening of CT interaction was also supported by the unusual change of the glass transition temperature (T_g) upon irradiation of UV light. As shown in **Figure 7**, T_g of hybrid film decreased along with the photodimerization of AN. Generally, T_g of polymer hybrid should be enhanced by the cross-linking induced by photodimerization of AN. The reasonable explanation to the unusual change of T_g is that the photodimerization of AN destroys the CT interaction, resulting in the weak interaction between two components PI and POSS-AN in hybrid film, and consequently leading to the decreasing T_g.

As the photodimerization of AN is reversible, the dimer of AN can change back to AN upon heating or irradiation of 254 nm UV light. After heating the photo-cross-linked hybrid film at 150 °C for 3 h, the UV–vis absorption (Figure S4, Supporting Information) and fluorescence emission around 650 nm (Figure 6, recovery) of sample 1-1 were almost restored to initial condition, suggesting the re-formation of the CT complex. These results proved that the reversible photodimerization of AN provides the ability to *on-off* control the CT interaction of PI and POSS-AN in hybrid films through heating and irradiation of light.

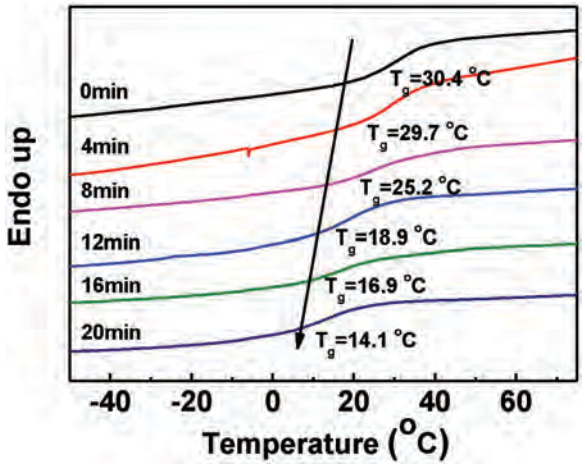

Figure 7. DSC curves of PI@POSS-AN/1-1 samples after irradiation of 365 nm UV light for different time. The scanning rate is 10 °C min^{-1} upon heating.

2.3. Photo-Rewritable Fluorescence Patterning

As the fluorescence emission of CT complex can be tuned by light and heat, photo-rewritable fluorescence pattern can be realized on our hybrid films, which might be potential in applications such as rewritable data storage and ultrahigh-resolution imaging. To probe this idea, we here demonstrated a reversible patterning strategy through photolithography based on the light-controllable CT interactions. The hybrid layer of PI@POSS-AN/1-1 was spinning-coated on the glass substrate, which was covered with a mask and then irradiated by 365 nm UV light. The resulting fluorescence micro-pattern was evaluated by confocal laser scanning microscopy (CLSM) through both green and red channels under a fixed wavelength (404 nm) of blue excitation.

As shown in **Figure 8**, the hybrid layer is red, which should be ascribed to fluorescence emission of CT complex. The formation of CT complex almost completely quenched the green fluorescence of NDI moieties. Upon irradiation, the exposed area of hybrid layer turns gradually from red to green, while the unexposed area kept red emission. The green emission in the exposed area should be attributed to the fluorescence of NDI moieties of PI. After irradiated for 10 min, the exposed area exhibited strong green fluorescence, suggesting that the CT complex was completely destroyed by the photodimerization of AN. Based on this strategy, a series of dual fluorescence micro-patterns with the tunable contrast can be obtained through the feasible and simple photolithography of one-step. Furthermore, the green emission of the exposed area can be erased by heating. After heating at 150 °C for 1 h, no micro-pattern can be observed and the whole layer became red again. This can be explained by that the AN dimers turned into AN after heating, resulting in the re-formation of CT complex with red emission. As the fluorescence pattern is erasable by controlling the CT interaction of NDI and AN, the photo-rewritable pattern can be realized on our hybrid film. As shown in **Figure 9**, dual fluorescence micro-pattern with different images was obtained on the same hybrid films through reversible process of photolithography-heating-photolithography. Taking "annulus" and "grid" mask for examples, the hybrid layer with the dual "annulus" micro-pattern turned into the single red color without pattern after heating at 150 °C. After irradiation of 365 nm UV light through "grid" mask, a dual "grid" micro-pattern was then obtained. To the best of our knowledge, this is the first example to realize the reversible fluorescence micro-pattern by the photo-controllable CT interaction.

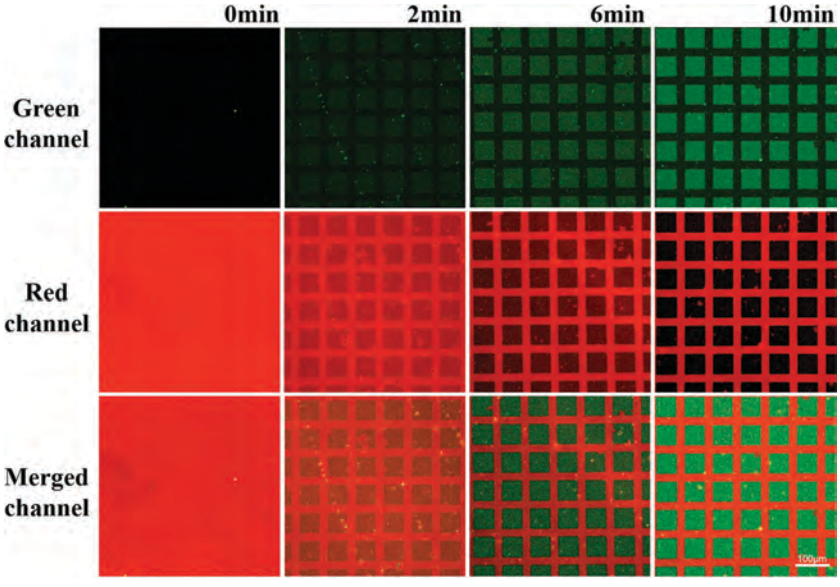

Figure 8. CLSM fluorescent images of sample PI@POSS-AN/1-1 after photolithography (365 nm UV light, copper mesh as mask) for different times. The pictures were taken through both green and red channels and the excitation wavelength of blue light for CLSM is fixed at 404 nm. Scale bars correspond to 100 μm.

2.4. Healing and Reprocessing of Cross-Linked Hybrid Film

Generally, cross-linking might bring some obvious advantages to polymer hybrids such as excellent mechanical and thermal performance and high resistance to chemicals, whereas cause difficulty in self-healing and reprocessing. By taking advantage of the reversible CT interaction and photodimerization of AN groups, we demonstrate that our cross-linked hybrid films of PI@POSS-AN can be self-healed and reprocessed under heating.

The hybrid film of PI@POSS-AN/1-1 was first cross-linked through the photodimerization of AN under irradiation of 365 nm UV light. After scratched with a knife (about 0.1 mm wide), the healing behavior of hybrid film was investigated by optical microscopy as well as uncross-linked film as reference. Upon heating at 50 °C, the scar on uncross-linked film became smaller gradually and disappeared completely after 40 min (Figure S5, Supporting Information). This might be ascribed to the strong CT interaction between NDI and AN. At the higher temperature than T_g, the strong intermolecular interaction makes the polymer chains with high mobility and fused together, resulting in the excellent performance of self-healing for uncross-linked film. On the other hand, the scratch on the cross-linked hybrid film remained remarkable even after heating at 50 °C for 4 h (Figure S5b, Supporting Information). Due to thermal expansion of polymer, the scratch became larger to a certain extent. These results are consistent with the fact that cross-linked materials are usually hard to heal.[33–35] As shown in **Figure 10**, however, the scar on the cross-linked hybrid film was hardly to be observed after heating at 150 °C for 1 h, suggesting the cross-linked film can be healed at the high temperature. Upon heating at 150 °C, AN was released from its dimer and the cross-linked film became uncross-linked. The strong CT interaction between NDI and AN was reformed in the hybrid film, allowing it to heal.

The cross-linked film was evaluated for their reprocessing ability via a reprocessing cycle monitored by tensile testing experiments. As shown in **Figure 11**a, the cross-linked

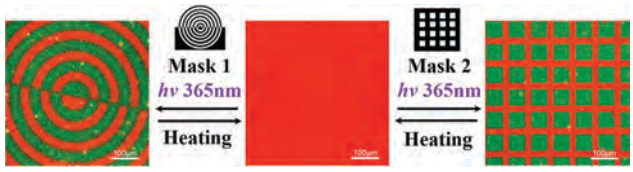

Figure 9. CLSM images of photo-rewritable fluorescence micro-pattern which were prepared on sample PI@POSS-AN/1-1, alternately overlay/removing masks ("grid" and "annulus") under 365 nm UV illumination. Erasure procedure was achieved by heating the patterned film at 150 °C for 1 h. The excitation wavelength of blue light for CLSM is fixed at 404 nm.

hybrid film that has been cut into pieces can be reprocessed and reshaped by compression molding at high temperature. 30 min of molding at 150 °C is enough to prepare a recycled object, which owns approximately the same tensile strength as the original one. After irradiation of UV light for 30 min, the reprocessed one was cross-linked again, and its tensile strength recovered to the original cross-linked samples as well.

To further evaluate the ability to reprocess, series of stress–strain experiments was done to examine the mechanical properties of hybrid films. Figure 11b shows the typical stress–strain curves of hybrid films and the resulting tensile moduli is summarized in Table S2 (Supporting Information). The pure PI is elastomeric with tensile moduli of 4.6 MPa. The incorporation of POSS-AN (≈20 wt%) greatly enhanced its tensile moduli to 451.4 MPa, which can be further reinforced 17% up to 527.8 MPa after photo-cross-linking. Compared with the original one, tensile moduli of the reprocessed cross-linked hybrid film decreased slightly. Overall, the healing and reprocessing merits endow our hybrids with long servicing life, energy efficiency, environmental friendly, and stability, overcame the difficulty that cross-linked polymer hybrids are generally hard to heal and reprocess.

3. Conclusion

In summary, we demonstrated a novel multifunctional polymer hybrid consisting of NDI containing PI and AN-ended POSS-AN, in which π-electron-poor NDI and π-electron-rich AN can form CT complexes. The CT interaction between NDI and AN can be tuned by the reversible photodimerization of AN through UV light and heating, which is key to realizing the multifunctionality of polymer hybrids. The CT interaction between NDI and AN can be *turn-off* through the photodimerization of AN, and then *turn-on* through heating upon 150 °C. The photo-controlled CT interaction can provide ability to fabricate the rewritable dual fluorescence micro-patterns with red and green

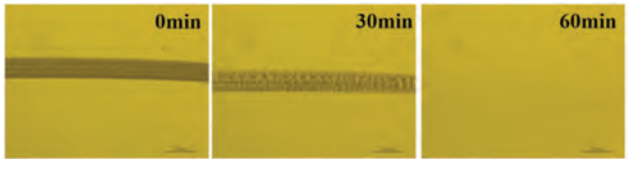

Figure 10. Optical microscope images of self-healing behavior of scratched cross-linked hybrid film PI@POSS-AN/1-1 at 150 °C. Scale bar is 100 μm.

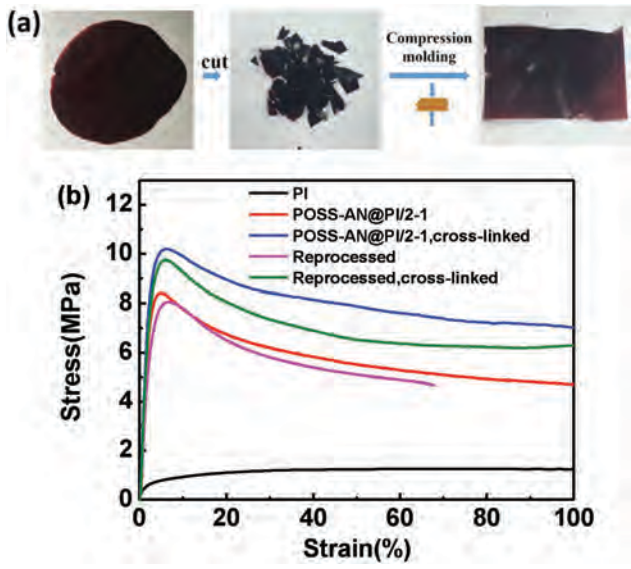

Figure 11. a) A cross-linked sample PI@POSS-AN/2-1 cut into pieces is reprocessed by compression molding; b) Stress–strain curves of pure PI, PI@POSS-AN/2-1, cross-linked PI@POSS-AN/2-1, reprocessed cross-linked PI@POSS-AN/2-1, and reprocessed cross-linked PI@POSS-AN/2-1 once again photo-cross-linked.

emission. Furthermore, the cross-linked polymer hybrids can be self-healing and reprocessed. It is the tunable CT interaction that brings the rewritable, healable, and reprocessing function to our polymer hybrids, which might find potential applications such as information storage and security.

4. Experimental Section

Materials: All solvents such as chloroform ($CHCl_3$), tetrahydrofuran (THF), hexane, ethanol, *N,N*-dimethylformamide (DMF), *N,N*-dimethylacetamide (DMAc), and toluene were purchased from Sinopharm Chemical Reagent. 1,4,5,8-Naphthalenetetracarboxylic dianhydride, 3-chloro-1,2-epoxypropane, and 3-aminopropyltriethoxysilane were purchased from Sinopharm. Jeffamine D-400 was purchased from Huntsman and 9-anthracenemethanol was purchased from Alfa Aesar. POSS-AN were synthesized according to a previous work.[36] All the reagents were used as received.

Synthetic Procedures: Synthesis of NDI Backbone Containing PI: NDI backbone containing PI was synthesized according to the literature.[17] Synthesis is summarized schematically in Scheme S1 (Supporting Information). The procedure for the preparation of the PI is as follows. A solution of Jeffamine D-400 (4.3 g, 10 mmol) in DMAc (10 mL) was added to a stirred suspension of 1,4,5,8-naphthalenetetracarboxylic dianhydride (2.68 g, 10 mmol) in DMAc (20 mL) and toluene (4 mL). Heating the suspension to 135 °C and the reaction became homogeneous. After 20 h, the reaction was ended and cooled to room temperature. Pour the dark solution into hexane (200 mL) to get the solid-state crude product. After washing with hexane for three times, the product was finally vacuum-dried at 80 °C overnight. The ^1H nuclear magnetic resonance (NMR) spectrum of PI is shown in Figure S6 (Supporting Information). The number-average molecular weight and the polydispersity index of PI ($M_n = 1.5 \times 10^4$, $M_w/M_n = 1.49$) was determined by gel permeation chromatography (GPC).

Sample Preparation: In this paper, the PI@POSS-AN hybrid samples are designated as *m-n*, where *m* and *n* stand for the molar ratio of NDI and AN moieties. For example, sample 1-1 represents the ratio of NDI and AN moiety in the hybrid is 1:1. Samples 1-0 and 0-1 represent

pure PI and pure POSS-AN, respectively. A series of PI/POSS-AN hybrid films were prepared by casting 20% wt $CHCl_3$ solution. After dried at 50 °C for 6 h to remove the solvents, the hybrid films with a thickness of about 0.3 mm were obtained, which can be further cross-linked by irradiation of 365 nm UV light with intensity of 10 mW cm^{-2}.

Reprocessing: The hybrid film PI@POSS-AN/2-1 was photo-cross-linked by UV irradiation for 60 min and then was cut into pieces. Pieces of cut sample were reprocessed by compression molding at 150 °C, under a pressure of 10 MPa. After 30 min, the resulting solid self-supported film was re-cross-linked by UV irradiation for tensile test.

Measurements: Nuclear Magnetic Resonance: NMR was acquired with a Mercury Plus spectrometer (Varian, Inc., USA) operating at 400 MHz and TMS as an internal standard at room temperature.

Gel Permeation Chromatography: GPC was carried out on an LC-20AD (Shimadzu, japan) system at 40 °C (50 µL injection column) with THF as the eluent solvent at a flow rate of 1.0 mL min^{-1}. The molecular weights and molecular weight distributions were determined by using polystyrene as the calibration standard.

UV–Vis Spectra: The UV–vis spectra were carried out with a UV-2550 spectrophotometer (Shimadzu, Japan). The samples were prepared by spin-coating method, which were also used for fluorescence spectra measurement.

Fluorescence Spectra: The fluorescence spectra were recorded using an LS-55B fluorescence meter (Perkin-Elmer, Inc., USA). The excitation wavelength is 385 nm.

Confocal Laser Scanning Microscopy: Fluorescence images of hybrids were viewed with a Leica TCS-SP5 LSCM (Leica, Germany) equipped with UV laser. After spin-coating the PI@POSS-AN/1-1 diluted solution (0.5 g/10 mL) on a tidy cover glass (20 × 20 × 0.15 mm), the samples were heated at 50 °C on an air-circulating oven for 10 min to remove all remaining solvent, and then combined with photolithograph to get patterns. Photomasks with hollowed out "grid" or "annulus" were designed and fabricated by Hatachi Chemical Co., Ltd.

Differential Scanning Calorimetry: DSC analysis was carried out with DSC 6200 (Seiko Instrument Inc.) at a heating rate of 10 K min^{-1} from 223 to 473 K and nitrogen flow rate of 50 mL min^{-1}.

Tensile: The tensile property of films was measured with an Instron 4465 instrument at room temperature with a humidity of about 30% at a crosshead speed of 20 mm min^{-1}. Noticeably, the films with a thickness of about 0.3 mm were cut into 4 × 30 mm for tensile measurement. Each datum was obtained from five parallel measurements.

Supporting Information

Supporting Information is available from the Wiley Online Library or from the author.

Acknowledgements

The authors thank the National Basic Research Program (2013CB834506) and National Nature Science Foundation of China (21274088, 51373098, and 21522403) for their financial support.

Received: March 18, 2016
Revised: April 14, 2016
Published online:

[1] C. Sanchez, B. Julian, P. Belleville, M. Popall, *J. Mater. Chem.* **2005**, *15*, 3559.
[2] C. Sanchez, K. J. Shea, S. Kitagawa, *Chem. Soc. Rev.* **2011**, *40*, 471.
[3] A. K. Cheetham, C. Rao, *Science* **2007**, *318*, 58.
[4] A. Kaushik, R. Kumar, S. K. Arya, M. Nair, B. Malhotra, S. Bhansali, *Chem. Rev.* **2015**, *115*, 4571.
[5] C. He, D. Liu, W. Lin, *Chem. Rev.* **2015**, *115*, 11079.
[6] J. Shi, Y. Jiang, X. Wang, H. Wu, D. Yang, F. Pan, Y. Su, Z. Jiang, *Chem. Soc. Rev.* **2014**, *43*, 5192.
[7] P. T. Yin, S. Shah, M. Chhowalla, K.-B. Lee, *Chem. Rev.* **2015**, *115*, 2483.
[8] R. Sharma, S. Sharma, S. Dutta, R. Zboril, M. B. Gawande, *Green Chem.* **2015**, *17*, 3207.
[9] C. Wan, X. Gu, F. Dang, T. Itoh, Y. Wang, H. Sasaki, M. Kondo, K. Koga, K. Yabuki, G. J. Snyder, *Nat. Mater.* **2015**, *14*, 622.
[10] C. Kagan, D. Mitzi, C. Dimitrakopoulos, *Science* **1999**, *286*, 945.
[11] F. Koppens, T. Mueller, P. Avouris, A. Ferrari, M. Vitiello, M. Polini, *Nat. Nanotechnol.* **2014**, *9*, 780.
[12] C. Sanchez, B. Lebeau, F. Chaput, J.-P. Boilot, *Adv. Mater.* **2003**, *15*, 1969.
[13] J. H. Heo, S. H. Im, J. H. Noh, T. N. Mandal, C.-S. Lim, J. A. Chang, Y. H. Lee, H.-J. Kim, A. Sarkar, M. K. Nazeeruddin, *Nat. Photonics* **2013**, *7*, 486.
[14] F. Hao, C. C. Stoumpos, D. H. Cao, R. P. Chang, M. G. Kanatzidis, *Nat. Photonics* **2014**, *8*, 489.
[15] N. J. Jeon, J. H. Noh, Y. C. Kim, W. S. Yang, S. Ryu, S. I. Seok, *Nat. Mater.* **2014**, *13*, 897.
[16] P. H. Ho, C. H. Chen, F. Y. Shih, Y. R. Chang, S. S. Li, W. H. Wang, M. C. Shih, W. T. Chen, Y. P. Chiu, M. K. Li, *Adv. Mater.* **2015**, *27*, 7809.
[17] S. Burattini, H. M. Colquhoun, J. D. Fox, D. Friedmann, B. W. Greenland, P. J. Harris, W. Hayes, M. E. Mackay, S. J. Rowan, *Chem. Commun.* **2009**, *44*, 6717.
[18] X. Zhang, Z.-C. Li, K.-B. Li, S. Lin, F.-S. Du, F.-M. Li, *Prog. Polym. Sci.* **2006**, *31*, 893.
[19] Y. H. Ko, E. Kim, I. Hwang, K. Kim, *Chem. Commun.* **2007**, *13*, 1305.
[20] A. Das, S. Ghosh, *Angew. Chem., Int. Ed.* **2014**, *53*, 2038.
[21] S. Burattini, B. W. Greenland, D. H. Merino, W. Weng, J. Seppala, H. M. Colquhoun, W. Hayes, M. E. Mackay, I. W. Hamley, S. J. Rowan, *J. Am. Chem. Soc.* **2010**, *132*, 12051.
[22] J. Fox, J. J. Wie, B. W. Greenland, S. Burattini, W. Hayes, H. M. Colquhoun, M. E. Mackay, S. J. Rowan, *J. Am. Chem. Soc.* **2012**, *134*, 5362.
[23] T. Ono, M. Sugimoto, Y. Hisaeda, *J. Am. Chem. Soc.* **2015**, *137*, 9519.
[24] M. Segura, L. Sánchez, J. de Mendoza, N. Martín, D. M. Guldi, *J. Am. Chem. Soc.* **2003**, *125*, 15093.
[25] R. M. K. Calderon, J. Valero, B. Grimm, J. de Mendoza, D. M. Guldi, *J. Am. Chem. Soc.* **2014**, *136*, 11436.
[26] S. V. Bhosale, C. H. Jani, S. J. Langford, *Chem. Soc. Rev.* **2008**, *37*, 331.
[27] A. Das, S. Ghosh, *Angew. Chem., Int. Ed.* **2014**, *53*, 1092.
[28] K. Tanaka, Y. Chujo, *J. Mater. Chem.* **2012**, *22*, 1733.
[29] D. Wang, J. Liu, J. F. Chen, L. Dai, *Adv. Mater. Interfaces* **2016**, *3*, 1500439.
[30] Z. Y. Jiang, Y. Zhou, L. Du, *Chin. J. Polym. Sci.* **2011**, *29*, 726.
[31] K. N. Raftopoulos, K. Pielichowski, *Prog. Polym. Sci.* **2016**, *52*, 136.
[32] P. Spenst, F. Würthner, *Angew. Chem., Int. Ed.* **2015**, *127*, 10303.
[33] D. Montarnal, M. Capelot, F. Tournilhac, L. Leibler, *Science* **2011**, *334*, 965.
[34] J. Bai, H. Li, Z. Shi, J. Yin, *Macromolecules* **2015**, *48*, 3539.
[35] P. Taynton, K. Yu, R. K. Shoemaker, Y. Jin, H. J. Qi, W. Zhang, *Adv. Mater.* **2014**, *26*, 3938.
[36] Z. Su, B. Yu, X. Jiang, J. Yin, *Macromolecules* **2013**, *46*, 3519.